

GMTalker: Gaussian Mixture-based Audio-Driven Emotional Talking Video Portraits

Yibo Xia*, Lizhen Wang, Xiang Deng, Xiaoyan Luo and Yebin Liu *Member, IEEE*,
<https://bob35buaa.github.io/GMTalker>

Abstract—Synthesizing high-fidelity and emotion-controllable talking video portraits, with audio-lip sync, vivid expressions, realistic head poses, and eye blinks, has been an important and challenging task in recent years. Most existing methods suffer in achieving personalized and precise emotion control, smooth transitions between different emotion states, and the generation of diverse motions. To tackle these challenges, we present GMTalker, a Gaussian mixture-based emotional talking portraits generation framework. Specifically, we propose a Gaussian mixture-based expression generator that can construct a continuous and disentangled latent space, achieving more flexible emotion manipulation. Furthermore, we introduce a normalizing flow-based motion generator pretrained on a large dataset with a wide-range motion to generate diverse head poses, blinks, and eyeball movements. Finally, we propose a personalized emotion-guided head generator with an emotion mapping network that can synthesize high-fidelity and faithful emotional video portraits. Both quantitative and qualitative experiments demonstrate our method outperforms previous methods in image quality, photo-realism, emotion accuracy, and motion diversity.

Index Terms—Facial Animation, Gaussian Mixture Model, Talking Video Portrait, Continuously Emotion Manipulation

I. INTRODUCTION

RECENTLY, audio-driven talking video portraits have drawn much research interest due to their broad applications in education, filmmaking, virtual digital human and entertainment industry, etc. It aims to produce audio-lip sync, photo-realistic, freely controllable video portraits given a driven speech. Actually, facial emotions and motions in other aspects, including head pose, eye blinks, and gaze, play a crucial role in generating photo-realistic and vivid video portraits. However, existing methods encounter challenges in achieving accurate and continuous emotional control, along with generating diverse motions and personalized speaking styles.

Previous methods [1]–[4] focus on audio-lip synchronization across different speakers, ignoring the control of facial emotion and motion generation. Some works pay attention to emotion control by either learning emotions from audio [5]–[7] or adding emotional source videos [8]–[11], which will introduce ambiguities. More recent methods [12]–[16] focus on generating emotional expressions that are consistent with the desired emotion label, providing a more reasonable and

controllable approach for synthesizing emotional talking video portraits. However, they still face challenges in achieving precise emotion control or continuously interpolating between different emotion states. This limitation stems from their approach of conditioning the emotion label into an emotion-agnostic framework through a one-hot vector (representing a discrete emotion space) [12]–[15] or deep emotional prompts (representing an entangled emotion space) [16] to implicitly learn the mapping between emotion and facial expression. None of these approaches can model a continuous and disentangled emotion space for better interpolation properties as well as more precise emotion control. To address this problem, we propose a Gaussian Mixture based Expression Generator (GMEG) which explicitly learns a conditional Gaussian mixture distribution among audio, emotion, and 3DMM expression coefficients. Our insight is to construct a continuous and disentangled latent space, where each Gaussian component represents specific emotional properties of the data, and these components are highly decoupled from each other. By leveraging this learned Gaussian mixture latent space, we achieve precise emotion control and smooth emotional transition.

Besides emotional facial expressions, the motion of other factors, such as head pose, eye blink, and gaze, are essential to the realism of synthesized videos. Some research [17]–[25] model the correspondence between audio and motion. However, they have not considered emotional control, and only a few works [6], [15] can control both emotion and motions simultaneously. Moreover, they encounter a so-called “mean motion” challenge, which means the synthesized motion tends to be over-smoothing and lacks diversity. To overcome their weakness, we propose a Normalizing Flow-based Motion Generator (NFMG), which enhances the motion prior by incorporating normalizing flow and learns the one-to-many mapping between the speech and motions. Moreover, to fully leverage the normalizing flow’s potential for fitting complex data distributions, we pre-train proposed NFMG on Vox2celeb2 [26] dataset with wide-range head and eye movements. In this way, we can obtain a more diverse motion prior and alleviate the “mean motion” issue. Additionally, our method can independently control expressions and motions by utilizing a parametric facial model [27].

Finally, existing methods [8], [15], [16] lack consideration for generating emotional portraits faithful to a specific person. To address this limitation, we introduce a stylized head generator, StyleUNet [28], which can reconstruct the personalized style of a target identity by the latent code. However, owing to the highly coupled latent space of StyleUNet, it struggles to

* Work done during an internship at Tsinghua University.

Lizhen Wang, Xiang Deng and Yebin Liu are with the Department of Automation, Tsinghua University, Beijing 100084, P.R.China.

Yibo Xia and Xiaoyan Luo are with the School of Astronautics, Beihang University, Beijing, 100191, P.R. China.

Corresponding author: Xiaoyan Luo.

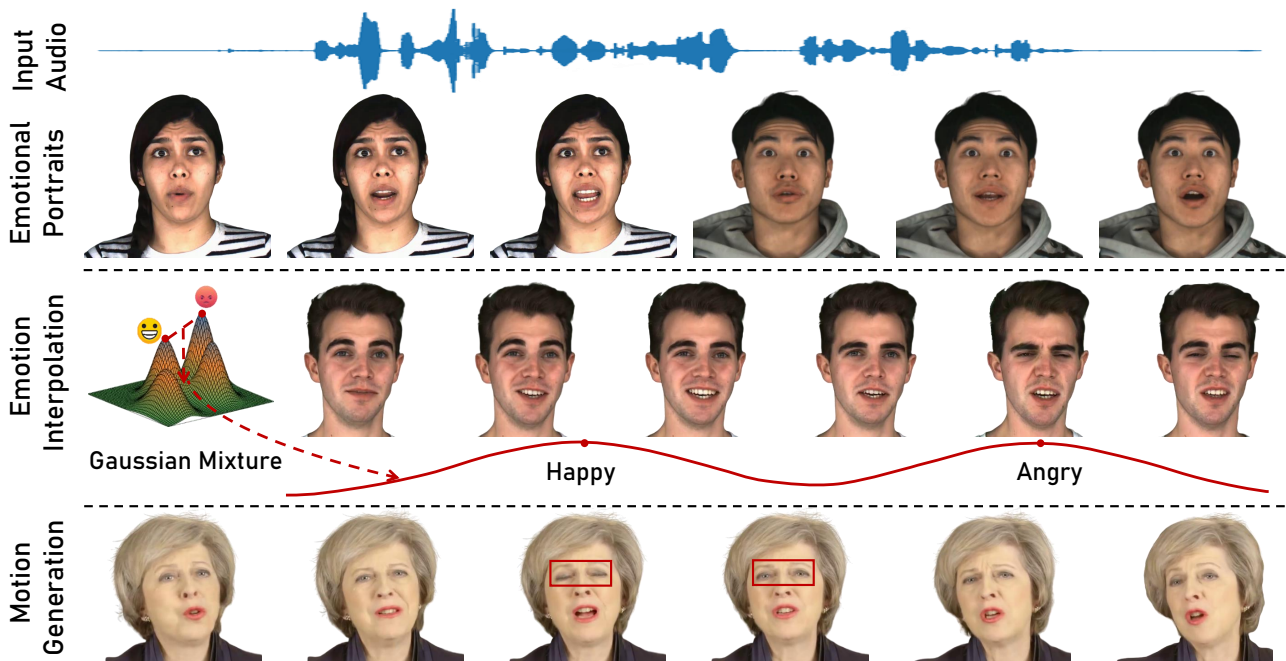


Fig. 1. GMTalker. Given the driving speech and emotion label, our method can generate high-fidelity and faithful emotional talking video portraits with diverse motions. Emotions can be freely manipulated within our continuous and disentangled Gaussian mixture distributed latent space. Additionally, our method can also predict motions from the input speech, including head poses, eye blinks, and gaze.

explicitly control the desired emotion. Therefore, we introduce an Emotion Mapping Network (EMN) to branch each emotion mode corresponding to the available sub-domain, which can control detailed emotion-related styles of the target person. Consequently, we can synthesize emotional portraits with personalized speaking styles.

We conduct comprehensive emotion interpolation comparison experiments, evaluating the smoothness and precision of the emotion transition from both quantitative and qualitative perspectives. Compared with other state-of-the-art methods, the proposed GMTalker shows smoother and more precise emotion transitions while maintaining accurate lip synchronization. Our main contributions can be summarized as follows:

- We propose a Gaussian mixture-based expression generator (GMEG) to disentangle different emotion states in continuous latent space, thereby achieving more precise emotion control and better interpolation properties.
- We present a normalizing flow-based motion generator (NFMG) pretrained on a large dataset with wide-range motions to generate diverse motion coefficients, including head poses, eye blinks, and gaze.
- We introduce a personalized emotion-guided head generator with an emotion mapping network (EMN) that can synthesize high-fidelity and faithful emotional video portraits with personalized speaking styles.

II. RELATED WORK

Most existing works can be roughly classified into digital 3D human faces [29]–[35] and realistic human portraits [1], [36]–[38], according to their output. The methods that animate

3D models of faces map the input speech to 3D mesh via carefully designed architecture. However, their applicability is limited due to the requirement for expensive 3D training data. Thus, we focus on generating photo-realistic talking video portraits.

a) Speech-Driven Talking Video Portraits: Most of the existing methods pay attention to generating movements in the mouth region [1]–[4], [39]–[45]. For instance, Wav2Lip [1] inpaints the lower half of the face using an expert SyncNet [46] to align the speech and mouth region. These lines of research, leaving the remaining video stationary, can only synthesize the lower half face. Other methods aim to generate the whole face by either wrapping the reference image according to input speech [22], [23], [47] or extracting face and audio features as a fused input to the decoder model [19], [48]–[50]. However, directly modeling the correspondence between audio and dynamic facial expressions in an end-to-end manner struggles to control head motion and synthesize high-quality face images.

Recently, with the development of 3D face reconstruction [27], [51], some works leverage explicit 2D/3D facial landmarks [20], [24], [36]–[38], [52], [53] or 3D face models [11], [17], [18], [21], [54]–[56] to reconstruct interpretable landmarks or face parameters, and then translate them to photo-realistic results. MakeItTalk [38] utilizes disentangled speech content and speaker identity features to animate the facial landmarks of a provided portrait. Benefiting from the controllability of 2D/3D representations, some methods [17], [18], [20], [21], [24], [56] achieve explicitly motion control, which makes the synthesized portraits more realistic. LSP [20] leverages a probabilistic autoregressive module to reconstruct

dynamic landmarks. SadTalker [56] designs an ExpNet and a PoseVAE to separately learn the expression and pose coefficients of 3DMM. Besides, recent work EMO [57] leverages the power of the diffusion model to directly generate video portraits with the controllable head motion from the input audio and a reference image, achieving excellent performance. However, none of them has considered emotional control which is a key factor in generating realistic portraits.

b) *Emotional Talking Video Portraits*: Emotion significantly impacts the realism of synthesized portraits. Recently, some works have paid attention to controlling the emotion of the output portraits. EAMM [8], GC-AVT [9], Styletalk [11], and PD-FGC [10] control emotion by external emotional source videos, inevitably introducing a semantic leakage problem. EVP [5], EMMN [6] directly identify emotion from labeled audio. However, determining emotions from input audio only may introduce ambiguities [8]. Other works ETK [12], MEAD [13], Sinha *et al* [14], SPACE [15], EAT [16] learn the inherent correspondence among emotion, audio, and facial expression implicitly via conditioning the emotion-agnostic network with emotion labels. However, none of them explicitly models a continuous and disentangled emotion space, leading to poor emotion interpolation properties and inaccurate emotion generation. Our method animates the emotion-controllable talking video portraits, including facial expression, head pose, blinks, and eye gaze.

III. METHOD

We present GMTalker, a Gaussian mixture-based audio-driven emotional video portrait generation framework taking the 3DMM as the intermediate representation. Given an audio and an emotion label as input, our system produces a talking video of a target person. It includes two generators for emotional expression coefficients and motion-related coefficients, as well as an emotion-guided head generator. The whole pipeline of our proposed method is illustrated in Fig 2. Specifically, we first extract per-frame 3DMM expression and motion coefficients by fitting a face parametric model (Section III-A). Then, we propose a Gaussian mixture expression generator (GMEG) in Section III-B to generate emotional 3DMM expression coefficients from an audio and emotion label by learning a Gaussian mixture latent space. Meanwhile, we present a normalizing flow-based motion generator (NFMG) in Section III-C to produce diverse head poses, gazes, and eye blink coefficients. Finally, we present an emotion-guided head generator with an Emotion Mapping Network (EMN) in Section III-D to generate photo-realistic emotional portraits with personalized speaking styles from the generated expression and motion coefficients.

A. Preliminary of 3D Head Representation

Given a T -frame emotional monocular portrait video of the target person, we first perform parametric model fitting to extract 3DMM coefficients as our intermediate representation and generate 3DMM renderings for training. We utilize FaceVerse [27] for the following reasons. First, the expression and shape bases of FaceVerse are rich and diverse, enabling it to effectively capture complex and emotion-related expressions

across different identities compared with other facial models [51], [58], [59]. Second, it excels in tracking stable head pose and capturing eyeballs and eye blinks. The 3D face shape of FaceVerse S can be formulated as:

$$S = \bar{S} + \gamma B_{shape} + \beta B_{exp}, \quad (1)$$

where \bar{S} is the mean shape, B_{shape} and B_{exp} are the bases of shape and expression. Expression coefficients $\beta \in \mathbb{R}^{169}$, blink coefficients $\theta_{blink} \in \mathbb{R}^2$, translation $t \in \mathbb{R}^3$, scale s , and the rotations of the head and two eyeballs $r_1 \in \mathbb{R}^3$, $r_2 \in \mathbb{R}^2$, $r_3 \in \mathbb{R}^2$ are optimized using differentiable renderer in [28] frame by frame. To generate identity-irrelevant coefficients, we only optimize shape coefficients $\gamma \in \mathbb{R}^{150}$ in the first frame for the target speaker following [28], [56], [60]. In the end, we obtained facial expression coefficients sequence $\{\beta\}_{t=1}^T$ rich in emotional information and motion coefficients sequence $\{\rho\}_{t=1}^T = \{[r_1, t], r_2, r_3, \theta_{blink}\}_{t=1}^T$ capable of representing realistic movements. In terms of audio processing, we employ a pretrained HuBERT model [61] to extract the audio feature $\{a\}_{t=1}^T$, following methods [62], [63].

B. Gaussian Mixture Expression Generator

Input with the audio and an emotion weight label, we propose a Transformer-based GMEG to generate emotional expression coefficients. We consider the audio-driven emotional expression generation as a conditional generation task and explicitly model the conditional distribution between the input audio feature $\{a\}_{t=1}^T$, emotion weight label e , and facial expression coefficients $\{\beta\}_{t=1}^T$. Since previous methods struggle to model a continuous and disentangled emotion space with better interpolation properties and more precise emotion control, we utilize a Gaussian mixture distribution to model the emotion latent space for expression generation, inspired by GMVAE [64]. Our insight is that the observed emotion data follows a Gaussian mixture distribution, and we restrict the distribution of the latent code to their corresponding emotion modes. This approach allows us to model a continuous and disentangled latent space, in which we can easily control emotion and smoothly interpolate between different emotion states.

1) *Preliminary*: Our GMEG can be mathematically formulated as a joint distribution:

$$p_{\beta, \theta}(\beta, z, w, e, a) = p(w)p(e)p_{\delta}(z|w, e)p_{\theta_{\beta}}(\beta|z, a), \quad (2)$$

which means our generative model will generate an observed expression coefficient β from the audio a , the latent variables w, z , and the emotion label e . Specifically, the latent variable w follows the normal distribution $w \sim \mathcal{N}(0, I)$, and the emotion label e follows the uniform distribution $e \sim \mathcal{U}(0, K)$, $p(e = k) = \pi_k = 1/K$, where K is the number of components in the mixture (i.e. the number of emotion types in datasets).

Then, by sample from w -space conditioned on various emotion e_k , we can model a conditioned Gaussian mixture distribution $z|e, w$ (i.e. Gaussian mixture latent space):

$$p_{\delta}(z|w, e) = \sum_{k=1}^K \pi_k \mathcal{N}(z; \mu_{\delta}^k(w), \Sigma_{\delta}^k(w)), \quad (3)$$

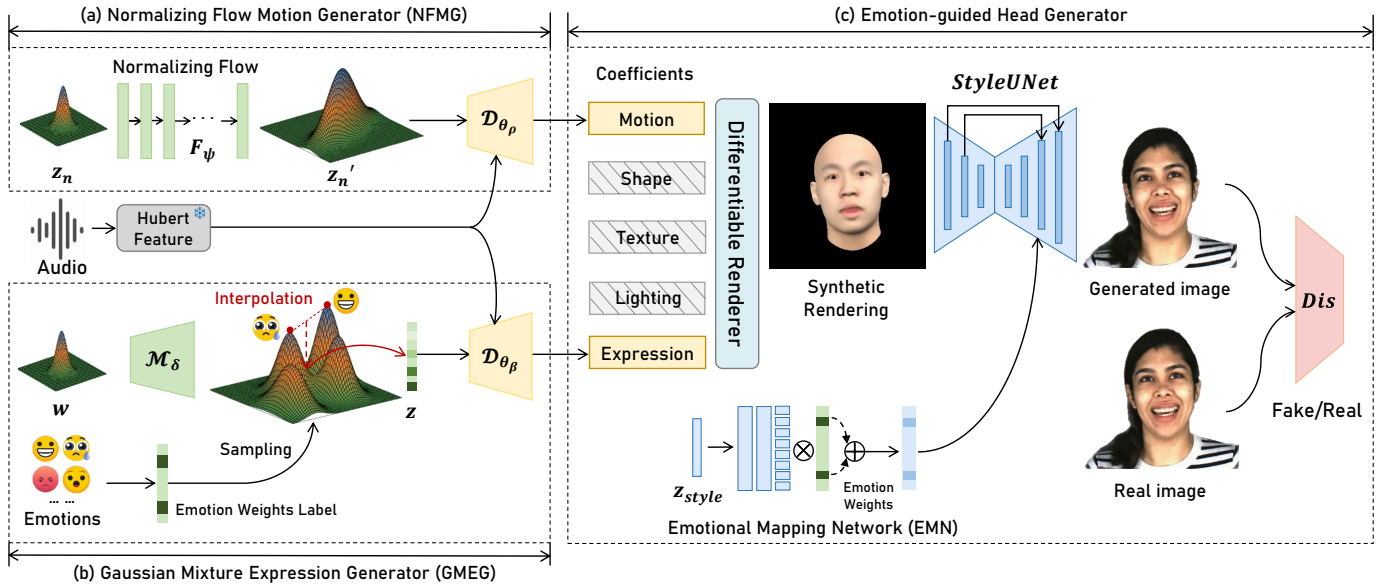


Fig. 2. Pipeline of GMTalker. Our framework consists of three parts: (a) In Section III-B, given the input speech and emotion weights label, we propose GMEG to generate 3DMM expression coefficients sampling from Gaussian mixture latent space. (b) In Section III-C, we introduce NFMG to predict motion coefficients from the audio, including poses, eye blinks, and gaze. (c) In Section III-D, we render these coefficients to 3DMM renderings for the target person and then use an emotion-guided head generator with EMN to synthesize photo-realistic video portraits with personalized style.

where μ_δ^k and Σ_δ^k represent a set of K means and variances of Gaussian mixture modeled by a neural network. Finally, we can generate expression coefficients $\beta_{1:t}$ by a decoder with latent variable z and audio $a_{1:t}$ as input.

2) *Architecture*: We employ a VAE [65] paradigm to learn the above Gaussian mixture latent space, which includes an encoder, a mixture-of-Gaussian (MoG) mapper, and a decoder. To capture long-range context dependencies and process arbitrary-length sequences, we further employ Transformer architectures [66] to model all of these networks and obtain sequence-level embeddings for both expression coefficients and audio features.

Encoder. As shown in Fig 3a, our Transformer-based encoder aims at learning two approximate posterior distributions: a normal distribution $q_{\phi_z}(z|\beta, a) = \mathcal{N}(z; \mu_{\phi_z}(\beta, a), \Sigma_{\phi_z}(\beta, a))$ and Gaussian mixture distribution $q_{\phi_w}(w|\beta, a) = \mathcal{N}(w; \mu_{\phi_w}(\beta, a), \Sigma_{\phi_w}(\beta, a))$, taking expression coefficients $\beta_{1:t}$ and audio features $a_{1:t}$ as input:

$$z, w = \mathcal{E}_\phi(\beta_{1:t}, a_{1:t}). \quad (4)$$

We first embed the input expression coefficients into a d -dimensional space via a linear projection. Then, we combine these projected features with audio features as the input of sinusoidal positional encoding to provide temporal order information periodically [66]. We use 8 Transformer encoder layers to model capture long-range context, followed by two average pooling layers to produce two groups of distribution parameters: μ_{ϕ_w} , Σ_{ϕ_w} , μ_{ϕ_z} and Σ_{ϕ_z} .

Mixture-of-Gaussian Mapper. To generate the conditioned Gaussian mixture distribution $p(z|w)$ from the latent variable w , we propose a Transformer-based MoG mapper with parameters δ , which consists of 8 Transformer encoder layers, without positional encodings. Our MoG mapper outputs a set

of K means μ_δ^k and variances Σ_δ^k of Gaussian mixture, written as:

$$\mu_\delta^k, \Sigma_\delta^k = \mathcal{M}_\delta(w). \quad (5)$$

Decoder. Given the latent variable z , audio feature $a_{1:t}$, and the personalized learnable embedding s_n of speaker n , we autoregressively generate emotional expression coefficients $\beta_{1:t}$ by a Transformer-based decoder parametrized by θ_β :

$$\hat{\beta}_t = \mathcal{D}_{\theta_\beta}(z, a_{1:t}, \hat{\beta}_{1:t-1}, s_n). \quad (6)$$

Our decoder consists of 8 Transformer decoder layers with a linear expression projection layer, where we add a latent variable z to a sequence of positional encodings as the Transformer input embeddings and then predict the current expression coefficient $\hat{\beta}_t$ conditioned on the previous expression coefficients $\hat{\beta}_{1:t-1}$. Notably, we enhance the Transformer decoder with causal self-attention to capture dependencies within the past expression coefficient sequence, and with cross-modal attention to align the audio and expressions, inspired by [31].

3) *Training Loss*: Due to the introduction of the Gaussian mixture prior, the optimization objective of VAE has some changes and no longer offers a simple analytical solution. Therefore, we optimize our GMEG using the log-evidence lower bound (ELBO) loss following [67], which can be written as:

$$\mathcal{L}_{exp} = \lambda_{rec}\mathcal{L}_{rec} + \lambda_{cond}\mathcal{L}_{cond} + \lambda_w\mathcal{L}_w + \lambda_{emo}\mathcal{L}_{emo}. \quad (7)$$

where λ_{rec} , λ_{cond} , λ_w , and λ_{emo} are loss weights. The gradients can be backpropagated via the reparameterization trick [65].

We refer to \mathcal{L}_{rec} as the reconstruction term, which can be also written as MSE loss between ground-truth and reconstructed expression coefficients: $\mathcal{L}_{rec} = \left\| \beta_{1:t} - \hat{\beta}_{1:t} \right\|_2$. The conditional regularizer \mathcal{L}_{cond} is proposed to push the

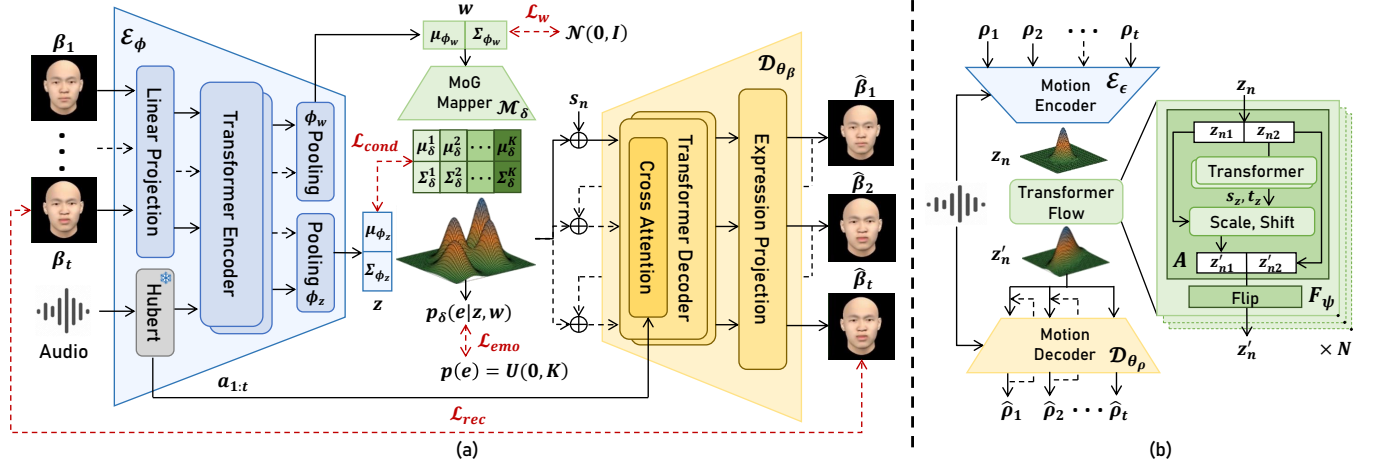


Fig. 3. The training process of our proposed GMEG and NFMG. (a) We autoregressively reconstruct facial expression coefficients $\hat{\beta}_{1:t}$ from input audio $a_{1:t}$ and emotion label e by optimizing four loss: \mathcal{L}_{rec} , \mathcal{L}_{cond} , \mathcal{L}_w , \mathcal{L}_{emo} . (b) Our NFMG generates diverse motions $\hat{\rho}_{1:t}$ from audio, including head poses, eye blinks, and gaze, by learning a Transformer normalizing flow-based VAE.

approximated posterior single Gaussian distribution near each emotion component of the Gaussian mixture prior. Since this term lacks a closed-form solution, we use the 1-step Monte Carlo samples to estimate the expectation over $q_{\phi_w}(w|\beta, a)$ and $q_{\phi_z}(z|\beta, a)$:

$$\begin{aligned} \mathcal{L}_{cond} &= \mathbb{E}_{q_{\phi_w}(w|\beta, a)q_{\phi_z}(z|\beta, a)} D_{KL}(q_{\phi_z}(z|\beta, a) || p_\delta(z|w, e)) \\ &= \frac{1}{N} \frac{1}{M} \sum_{n=1}^N \sum_{m=1}^M \sum_{k=1}^K \tilde{\pi}_k \log \frac{q_{\phi_z}(z_m | \beta, a)}{p_\delta(z_m | w_n, e = k)} \\ &= \log q_{\phi_z}(z | \beta, a) - \sum_{k=1}^K \tilde{\pi}_k \log p_\delta(z | w, e = k) \end{aligned} \quad (8)$$

where $\tilde{\pi}_k$ is the posterior distribution of emotion derived from z and w :

$$\tilde{\pi}_k = p_\delta(e = k | z, w) = \frac{\pi_j \mathcal{N}(z; \mu_\delta^j(w), \Sigma_\delta^j(w))}{\sum_{k=1}^K \pi_k \mathcal{N}(z; \mu_\delta^k(w), \Sigma_\delta^k(w))} \quad (9)$$

\mathcal{L}_w is the regularizer of normal distribution w which reduces KL divergence between the normal posterior and the normal prior distribution as same as vanilla VAE, formulated as:

$$\begin{aligned} \mathcal{L}_w &= D_{KL}(q_{\phi_w}(w|\beta, a) || p(w)) \\ &= -\frac{1}{2} (\log \sigma_{\phi_w}^2 - \mu_{\phi_w}^2 - \sigma_{\phi_w}^2 + 1) \end{aligned} \quad (10)$$

\mathcal{L}_{emo} is the regularizer of emotion which reduces the KL divergence between the e -posterior and the uniform prior by pushing the same emotion samples generated from the same component of the Gaussian mixture, which can be written as:

$$\begin{aligned} \mathcal{L}_{emo} &= \mathbb{E}_{q_{\phi_z}(z|\beta, a)q_{\phi_w}(w|\beta, a)} [D_{KL}(p_\delta(e|z, w) || p(e))] \\ &= \frac{1}{M} \sum_{i=1}^M D_{KL}(p_\delta(e|z_i, w_i) || p(e)) \\ &= \sum_{k=1}^K \tilde{\pi}_k (\log \tilde{\pi}_k + \log K), \end{aligned} \quad (11)$$

where we also use 1-step Monte Carlo samples to estimate the expectation over $q_{\phi_z}(z|\beta, a)$ and $q_{\phi_w}(w|\beta, a)$.

4) *Inference and Emotion manipulation*: In the inference stage, we predict emotional expression coefficients according to audio feature $a_{1:t}$, target emotion label e_{tar} , and personalized code s_n in an autoregressive manner. As shown in Fig 2, we first sample w from prior normal distribution $\mathcal{N}(0, I)$. Then, our MoG mapper generates a latent code z_{tar} corresponding to the target emotion, followed by the expression decoder to predict the final expression coefficients.

Benefiting from the continuous and disentangled Gaussian mixture latent space, our method can achieve emotion manipulation by mixing the different Gaussian latent codes corresponding to each emotion. Specifically, as shown in Fig 1, given the ‘‘happy’’ emotion e_1 and the ‘‘angry’’ emotion e_2 , we generate each latent code z_1 and z_2 through the MoG mapper determined by sampled w and its emotion label. Then, we can easily blend these two latent codes by changing the interpolation weight α :

$$z_{12}^\alpha = \alpha \mathcal{N}(z; \mu_\delta^1(w), \Sigma_\delta^1(w)) + (1 - \alpha) \mathcal{N}(z; \mu_\delta^2(w), \Sigma_\delta^2(w)) \quad (12)$$

C. Normalizing Flow based Motion Generator

Predicting head poses, eye blinks, and gaze from input audio is particularly challenging due to the one-to-many mapping between audio and motion. Besides, existing methods encounter the ‘‘mean motion’’ problem which means the synthesized motion tends to be over-smoothing, lacking diversity, and appearing blurred in the case of wide-range head movements. Previous work [56] utilizes simple distribution as the prior of VAE to predict head motion from audio, often causing the encoder to generate mean motion latent code. To enhance the complexity of the prior distribution, inspired by [62], [68], [69], we propose NFMG, a normalizing flow-based motion generator, to address these problems.

Given the input audio $a_{1:t}$, we utilize a normalizing flow to map normal distributions z_n to a more complicated distribution

z'_n and then decode the latent to motion-related coefficients $\{\rho\}_{t=1}^T \in \mathbb{R}^{12}$. This process can be written as follows

$$p_\psi(z'_n) = p(z_n) \left| \det \frac{\delta F_\psi}{\delta z_n} \right|, \quad p(z_n) \sim \mathcal{N}(0, I) \quad (13)$$

$$p_{\psi, \theta_\rho}(\rho, z_n, a) = p_\psi(z'_n) p_{\theta_\rho}(\rho | z'_n, a), \quad (14)$$

where ψ and θ_ρ are the model parameters of normalizing flow F_ψ and decoder $\mathcal{D}_{\theta_\rho}$.

Architecture. Our NFMG comprises a motion encoder, a Transformer normalizing flow, and a motion decoder. The motion encoder \mathcal{E}_ϵ and motion decoder $\mathcal{D}_{\theta_\rho}$ closely resemble the encoder and decoder of GMEG, with the encoder featuring only one linear layer to approximate the posterior distribution $q_\epsilon(z_n | \rho, a)$. To enhance the prior distribution of motion, we introduce a Transformer flow F_ψ , which is constructed by a series of N invertible Transformer-based nonlinear mappings $F_\psi = F_{\psi_1}(F_{\psi_2}(\dots F_{\psi_N}))$ parameterized by $\psi = \{\psi_n\}_{n=1}^N$. Specifically, each component mapping F_{ψ_n} contains two sub-steps: an affine coupling layer (A) and a flip operation. Given the latent $z_n = [z_{n1}, z_{n2}]$, the affine coupling layer aims to affinely transform half of the input elements z_{n1} based on the values of the other half z_{n2} [70]. To employ a more powerful nonlinear transformation, we utilize 4 Transformer encoder layers as our affine coupling layer to calculate the scale s_z and shift t_z of z_{n1} , which is different from existing works [69], [71], [72]. The flip operation ensures that after a sufficient number of flow steps, all variables can be nonlinearly transformed by reversing the ordering of the features.

Training. We utilize ELBO loss to train our NFMG. Additionally, we introduce a velocity loss to constraint temporal consistency. The loss function can be formulated as:

$$\begin{aligned} \mathcal{L}_m(\epsilon, \psi, \phi_\rho) &= \mathbb{E}_{q_\epsilon(z'_n | \rho, a)} [\log p_{\theta_\rho}(\rho | z'_n, a)] \\ &\quad - D_{KL}(q_\epsilon(z'_n | \rho, a) || p_\psi(z'_n)) \\ &= \|\rho_{1:t} - \hat{\rho}_{1:t}\|_2 \\ &\quad - \mathbb{E}_{q_\epsilon(z'_n | \rho, a)} [\log q_\epsilon(z'_n | \rho, a) - \log p_\psi(z'_n)] \end{aligned} \quad (15)$$

where the expectation of $q_\epsilon(z'_n | \rho, a)$ can be estimated by Monte-Carlo method.

However, merely incorporating normalizing flow proves inadequate for generating diverse motions across different data distributions. This is due to the motion acquired from a single video is usually insufficient for synthesizing diverse movements. Therefore, we pre-train our NFMG on VoxCeleb2 [26], a large dataset with diverse head and eye movements, to enhance the generalization of motion. So that we can make full use of the potential of the normalizing flow to fit complex data distributions and alleviate the ‘‘mean head motion’’ problem.

Inference. As shown in Fig 3b, our Transformer flows first map a latent variable z_n sampled from the prior normal distribution into z'_n . Then we pass this latent variable with input audio feature $a_{1:t}$ into our motion decoder to generate diverse and realistic motion coefficients $\hat{\rho}_{1:t}$ autoregressively similar to Section III-B. Since the z_n is randomly sampled, we can generate different head poses, eye blinks, and gazes given the same speech. Furthermore, we can also generate diverse and realistic motions given the different audio due to the powerful generative ability of the proposed NFMG.

D. Emotion-guided Head Generator

After generating emotional expression and other motion coefficient sequences from input audio (Section III-B and Section III-C), we render them to images using the fixed shape and texture coefficients of the target person (Section III-A). Next, we will generate photo-realistic images from synthetic 3DMM renderings through an image-to-image translation generator. We utilize the style-based generator, StyleUNet [28], which can reconstruct the personalized style of a target identity. However, owing to the highly coupled latent space of StyleUNet, it struggles to explicitly control the emotion that we want. Therefore, we introduce an Emotion Mapping Network (EMN) to branch each emotion type corresponding to the available sub-domain, motivated by [73].

Emotion Mapping Network. Given a latent code z_{style} and an emotion label, our EMN generates a style code $s_{style} = \mathcal{M}_k(z_{style})$, where $\mathcal{M}_k(\cdot)$ denotes the output corresponding to the emotion type k , and \mathcal{M} consist of an MLP with two shared layers and K multiple unshared layers (similar to the emotion numbers). To achieve more stable results, we incorporate a shoulder mask as an additional input different from StyleUNet. These shoulder masks are concatenated with the corresponding frames of the 3DMM renderings and together serve as input to the network. During the driving phase, stable shoulder motion is achieved by providing a reference shoulder mask image. Consequently, we can utilize z_{style} to control emotion-related details (such as facial wrinkles and hair) and background information, while maintaining stable shoulder positioning.

Training Loss. The emotion-guided head generator is trained in an adversarial way with a discriminator, which keeps the same architecture with the discriminator of StyleGAN2 [74]. During the training process, input with a single synthetic 3DMM rendering and an emotion label, we generate an output image. This output image is then concatenated with the 3DMM rendering as a 6-channel ‘‘fake’’ input for the discriminator. The corresponding ground-truth image and 3DMM rendering are concatenated into ‘‘real’’ input. As a result, we train our emotion-guided head generator using common L1 loss \mathcal{L}_1 , perceptual loss \mathcal{L}_{per} , and GAN loss \mathcal{L}_{GAN} following [28], which can be formulated as:

$$\mathcal{L}_{render} = \mathcal{L}_1 + \mathcal{L}_{per} + \mathcal{L}_{GAN} \quad (16)$$

IV. EXPERIMENTS

In this section, we first describe the experimental setup of our approach in Section IV-A: implementation details, dataset, baseline method, and evaluation metrics. Subsequently, we present the comparison results both qualitatively and quantitatively in Section IV-B. Finally, We show the results of a user study in Section IV-C and the ablation study in Section IV-D.

A. Experimental Setup

Dataset and Implementation Details. We conduct emotional experiments on the commonly used talking head datasets, MEAD [13] and CREMA-D [75]. MEAD is a high-quality emotional talking video dataset with 8 kinds of emotions and audio-visual recordings performed by different actors.

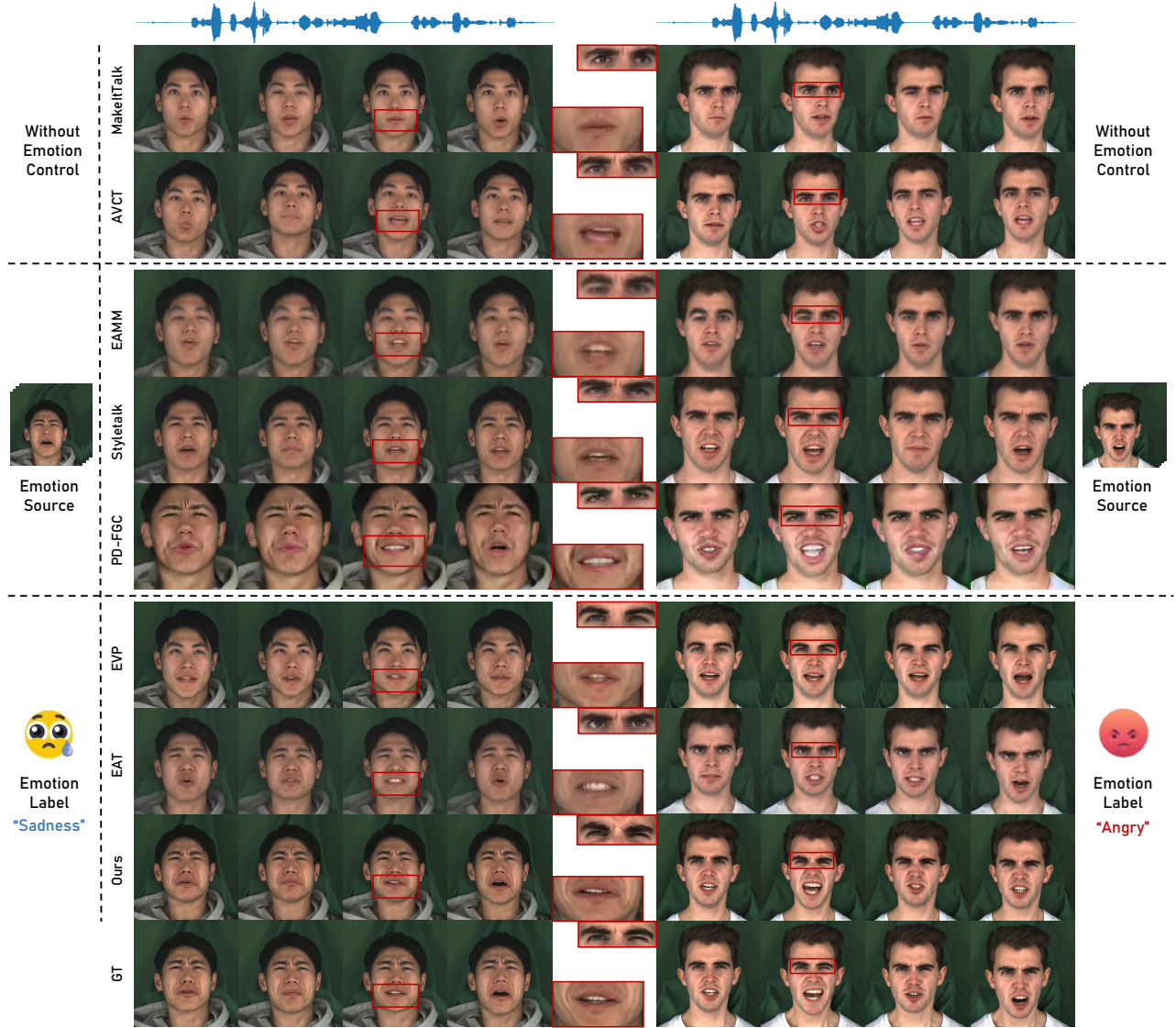


Fig. 4. Qualitative comparison for emotional talking video portraits on the two cases in the MEAD test dataset. From top to bottom: MakeItTalk [38], AVCT [23], EAMM [8], Styletalk [11], PD-FGC [10], EVP [5], EAT [16], our GMTalker, and ground truth. The emotion categories of the videos are happy (left) and angry (right). The bottom row shows ground-truth frames. Since EAMM [8] and EAT are one-shot methods, we choose the same reference image used in EAT [16] to generate target videos for them.

CREMA-D contains video clips of a variety of different age groups and races uttering 12 sentences expressing six categorical emotions. We train and test our model on 6 subjects for the MEAD dataset and 10 subjects for the CREMA-D dataset. As for non-emotional target-person experiments, we utilize the video samples from LSP [20] with 80%/20% for training and testing. Notably, we set the component of our Gaussian mixture K to 1 for non-emotional experiments, representing a normal distribution. Similarly, the number of unshared layers in EMN is set to 1. All the videos are sampled in 25 FPS and the audio sample rate is 16KHz. The MEAD and CREMA-D videos are cropped and resized to 512×512 and 256×256 , while the LSP dataset remains 512×512 .

We train our GMEG for 100 epochs taking about 8-10 hours using Adam optimizer where the learning rate is 1×10^4 , beta1 is 0.9 and beta2 is 0.999. For loss weights in Equation (7), we empirically set the loss weight λ_{rec} as 1.0, and λ_w, λ_{emo} ,

λ_{cond} as 0.5. To learn diverse and large motion changes, we select about 20k videos from the VoxCeleb2 [26] to pre-train our NFMG. Then, we fine-tune this diverse motion prior to a specific person taking a few minutes. We use the same hyperparameter settings with [28] to train the emotion-guided head generator on a specific person for about 4-6 hours. All experiments are conducted on an NVIDIA 3090 GPU.

Baseline. We compare our method with: (1) emotion-agnostic talking video generation methods: MakeItTalk [38], Wav2Lip [1], and AVCT [23]. (2) emotion-controllable talking video generation methods: EAMM [8], Styletalk [11], PD-FGC [10], and EAT [16]. Besides, we additionally compare our results on the CREMA-D dataset with Vougioukas et al [76], Diffused Heads [77] and ETK [12]. For motion-controllable talking video generation, we compare our method with several state-of-the-art motion-controllable methods: FACIAL [21], LSP [20], Audio2Head [22] and SadTalker [56], focusing on high-quality portrait generation with natural and

TABLE I
 QUANTITATIVE COMPARISONS WITH THE STATE-OF-THE-ART METHODS ON MEAD [13]. PLEASE NOTE THAT THE SYNC VALUE FOR EMOTIONAL TALKING VIDEO PORTRAITS MAY BE INACCURATE AS THE SYNCNET MODEL IS TRAINED ONLY WITH NEUTRAL VIDEOS.

Method	Emo Source	Visual Quality			Lip Synchronization			Emo Accuracy	Output		
		PSNR↑	SSIM↑	FID↓	Sync↑	M-LMD↓	F-LMD↓	Acc _{emo} ↑	Pose	Eye	Emo
MakeItTalk [38]	N./A.	18.79	0.55	51.88	5.28	3.61	4.00	15.23	generate	✗	✗
Wav2Lip [1]	N./A.	19.12	0.57	67.49	8.97	3.11	3.71	17.87	✗	✗	✗
AVCT [23]	N./A.	18.43	0.54	39.18	6.02	3.82	4.33	15.64	generate	✗	✗
EAMM [8]	Video	20.55	0.66	22.38	6.62	2.19	2.55	49.85	transfer	✗	✓
Styletalk [11]	Video	19.27	0.64	49.73	5.29	2.67	3.45	45.41	transfer	✗	✓
PD-FGC [10]	Video	20.97	0.65	39.52	6.29	1.80	2.15	36.09	transfer	transfer	✓
EAT [16]	Label	21.75	0.68	19.69	8.28	2.25	2.47	75.43	transfer	✗	✓
GMTalker (Ours)	Label	24.86	0.80	13.49	7.34	1.23	1.48	83.92	generate	generate	✓
Ground Truth	N./A.	∞	1.00	0	7.76	0.00	0.00	84.37	-	-	-

TABLE II
 QUANTITATIVE COMPARISONS WITH THE STATE-OF-THE-ART METHODS ON CREMA-D [75].

Method	Emo Source	Visual Quality			Lip Synchronization			Emo Accuracy	Output		
		PSNR↑	SSIM↑	FID↓	Sync↑	M-LMD↓	F-LMD↓	Acc _{emo} ↑	Pose	Eye	Emo
MakeItTalk [38]	N./A.	21.98	0.67	29.99	3.42	3.08	3.27	17.21	generate	✗	✗
Vougioukas et.al [76]	N./A.	22.11	0.68	34.93	5.01	2.10	2.63	26.81	✗	✗	✗
AVCT [23]	N./A.	20.65	0.63	23.69	5.42	2.87	3.77	14.87	generate	✗	✗
Diffused Heads [77]	N./A.	22.16	0.68	20.49	5.13	2.31	2.91	28.54	✗	✗	✗
EAMM [8]	Video	21.21	0.66	39.00	3.75	2.64	3.16	21.12	transfer	✗	✓
Styletalk [11]	Video	23.78	0.75	13.98	3.55	2.08	2.10	52.32	transfer	✗	✓
PD-FGC [10]	Video	23.82	0.73	24.86	4.77	1.55	1.85	46.22	transfer	transfer	✓
ETK [12]	Label	23.34	0.72	18.08	5.42	1.81	2.43	63.05	✗	✗	✓
EAT [16]	Label	21.66	0.66	20.78	5.78	2.62	2.89	46.09	transfer	✗	✓
GMTalker (Ours)	Label	24.16	0.77	9.24	6.80	1.43	1.59	82.91	generate	✓	✓
Ground Truth	N./A.	∞	1.00	0	7.76	0.00	0.00	98.42	-	-	-

diverse motion.

Evaluation Metrics. We use the following metrics to measure the visual quality and audio-visual synchronization for all quantitative experiments. For emotional talking video comparison, we employ Acc_{emo} to assess the emotional accuracy of synthesized videos. To measure the diversity of generated head motion, we adopt Beat Alignment (**BA**) and Diversity (**Div**) metrics used in SadTalker [56], as well as Percent of Correct Motion (**PCM**) mentioned in BEAT [78].

Audio-visual synchronization. We use the lip sync confidence score (**Sync**) of SyncNet [46] and the distance between the landmarks of the mouth (**M-LMD**) [37] for lip-sync evaluation. Furthermore, we measure the distance between the landmarks of the whole face (**F-LMD**) [8] to evaluate the accuracy of the pose and facial expressions.

Visual quality. We use **PSNR**, **SSIM**, and Frchet Inception Distance score (**FID**) to measure the image quality of synthesized video portraits.

Emotional accuracy. To quantify the accuracy of the synthesized emotional video, We utilize the same emotion classifier mentioned in [16] for the MEAD dataset. For the CREMA-D dataset, we train the same classifier used in [12] on the CREMA-D training set (total 76 identities).

Motion Diversity. To evaluate the diversity and richness of generated head motions, following in [56], we calculate the

distance between various predicted 3-dimension head motion embeddings extracted by TokenHPE [79], which can be defined as:

$$Div = \frac{2}{B \times (B - 1)} \sum_{i=1}^{B-1} \sum_{j=i+1}^B |\hat{m}_i - \hat{m}_j|_1, \quad (17)$$

where \hat{m}_i and \hat{m}_j are the i -th and j -th head motion embeddings in a batch B .

For the alignment of the audio and generated motions, we compute the beat align score proposed by [80]. **BA** measures the average distance between each motion beat and its nearest corresponding audio beat:

$$BA = \frac{1}{|B^m|} \sum_{b_j^m \in B^m} \exp\left\{-\frac{\min_{b_j^a \in B^a} |b_j^m - b_j^a|^2}{2\sigma^2}\right\}, \quad (18)$$

where $B^m = \{b_i^m\}$ and $B^a = \{b_i^a\}$ denotes the motion beats and audio beats, respectively. Following [78], [80], we set the normalized parameter σ as 3 in our experiment.

Besides, to measure the accuracy of predicted head motion, we compute the percentage of correctly predicted motion embeddings instead of keypoints, which can be calculated as:

$$PCM = \frac{1}{T \times J} \sum_{t=1}^T \sum_{j=1}^J \mathbf{1} \left[\left| \hat{m}_t^j - m_t^j \right|_2 < \tau \right], \quad (19)$$

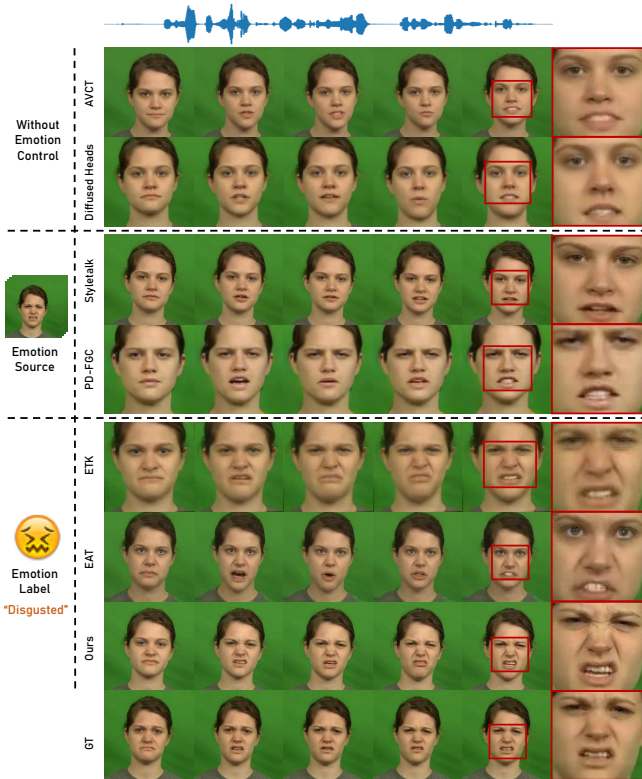


Fig. 5. Qualitative comparison for emotional talking video portraits on the CREMA-D [75] test dataset. From top to bottom: AVCT [23], Diffused Heads [77], Styletalk [11], PD-FGC [10], ETK [12], EAT [16], our GMTalker, and ground truth. The emotion category of the videos is anger. The bottom row shows ground-truth frames.

where $J = 3$ and \hat{m}_t^j, m_t^j are the j -th dimension of predicted motion embeddings and the ground-truth motion embeddings at the t -th frame. We only calculate the successfully recalled motion embeddings against a specified threshold $\tau = 1.0$.

B. Comparison Results

Comparison of Emotion Generation. For quantitative comparison, we adopt the experimental setup and evaluation method utilized by EAT [16] on the public-available MEAD and CREMA-D test set. As shown in Table I and Table II, GMTalker achieves the best overall visual quality and emotion accuracy, demonstrating the superior quality of disentangled emotion latent space learned by GMEG. In terms of the **Sync** score, our method shows comparable performance with other methods. Please note that a higher sync score does not invariably guarantee better results, as this metric can be overly sensitive to audio and the SyncNet model is trained only on neutral videos. The higher scores achieved by Wav2Lip [1] and EAT [16] may be attributed to their overfitting of the pretrained SyncNet model or utilizing synchronization loss.

Moreover, we make qualitative comparisons with several state-of-the-art methods on the sequences of the MEAD and CREMA-D test set. Illustrated in Fig 4 and Fig 5, our method excels in generating high-fidelity and faithful emotional talking video portraits. Specifically, while these methods either fail to express desired emotion or present mouth region artifacts, GMTalker remains comparatively more faithful to the original expression of the ground truth, including natural mouth shapes

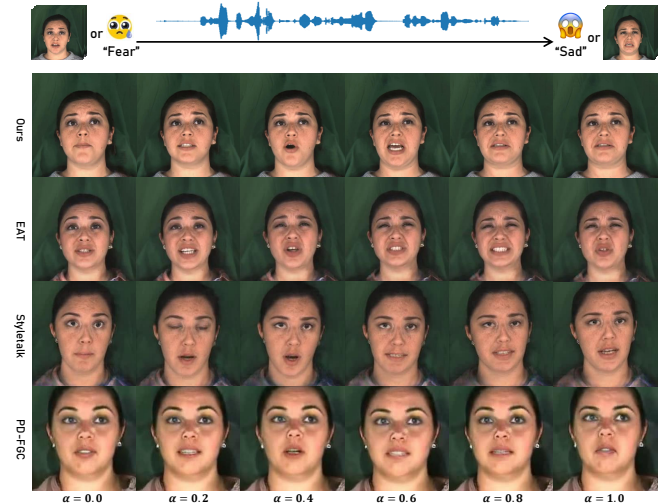


Fig. 6. Qualitative results of the emotion interpolation comparison. For PD-FGC [10] and Styletalk [11], we manipulate expressions between the source emotion video and the target emotion video. For EAT [16], we achieve this by transitioning between the source emotion label and the target emotion label.

TABLE III
QUANTITATIVE COMPARISON OF THE EMOTION INTERPOLATION STUDY.

Method	Emo Source	E-PPL↓	E-PDV↓	Sync↑
PD-FGC [10]	Video	21.08	44.95	5.30
Styletalk [11]	Video	12.84	15.35	5.61
EAT [16]	Label	8.89	7.28	6.64
Ours	Label	6.64	6.86	6.74

aligned with the input speech. Moreover, it can generate detailed expressions with personalized speaking styles, such as wrinkles in the face and eye regions.

Comparison of Emotion Interpolation. To illustrate the continuity and decoupling characteristics of our Gaussian mixture latent space learned by GMEG, we conduct an emotion interpolation study from both qualitative and quantitative perspectives, comparing our GMTalker with several state-of-the-art methods: EAT [16], Styletalk [11] and PD-FGC [10]. As shown in Fig 6, given the same driving audio, we obtain the image sequences of different methods by interpolating between the corresponding emotion features extracted from the source emotion “Fear” and the target emotion “Sad”. For Styletalk and PD-FGC, whose emotion features are extracted from the additional emotion videos, the generated facial emotion dynamics are not smoothly transformed and fail to perform the desired emotion transitions. For Styletalk and PD-FGC, which extract emotion features from additional emotion videos, the generated facial emotion dynamics lack smooth emotion transition and fail to achieve the desired emotion states. EAT generates emotional embeddings through its deep emotional prompts, resulting in relatively continuous facial expression dynamics. However, it may present ambiguous emotional states: the generated target expression “Sad” more closely resembles confusion or fear. In contrast, by interpolating in our continuous and disentangled Gaussian mixture latent space, we can smoothly transition from the source expression to the target expression while preserving the accuracy of the emotion.

To quantitatively evaluate the quality of intermediate facial

TABLE IV

QUANTITATIVE COMPARISONS WITH STATE-OF-THE-ART POSE-CONTROLLABLE METHOD ON LSP [20] TEST SAMPLES. WE EVALUATE SADTALKER [56] IN THE ONE-SHOT SETTINGS, AND OTHERS IN PERSON-SPECIFIC SETTINGS.

Method	Visual Quality			Lip Synchronization			Motion Diversity		
	PSNR \uparrow	SSIM \uparrow	FID \downarrow	Sync \uparrow	M-LMD \downarrow	F-LMD \downarrow	BA \uparrow	Div \uparrow	PCM \uparrow
FACIAL [21]	19.22	0.62	35.14	3.99	1.82	2.83	0.242	2.182	0.411
LSP [20]	19.48	0.62	46.45	4.93	1.99	2.84	0.252	2.173	0.432
Audio2Head [22]	16.97	0.53	56.06	6.94	2.47	3.89	0.259	2.182	0.433
SadTalker [56]	17.23	0.54	50.15	7.82	2.51	3.84	0.263	1.934	0.408
Ours	19.80	0.64	30.91	7.82	1.79	2.75	0.290	2.201	0.449
Ground Truth	∞	1.00	0	8.53	0.00	0.00	0.271	2.151	0.435

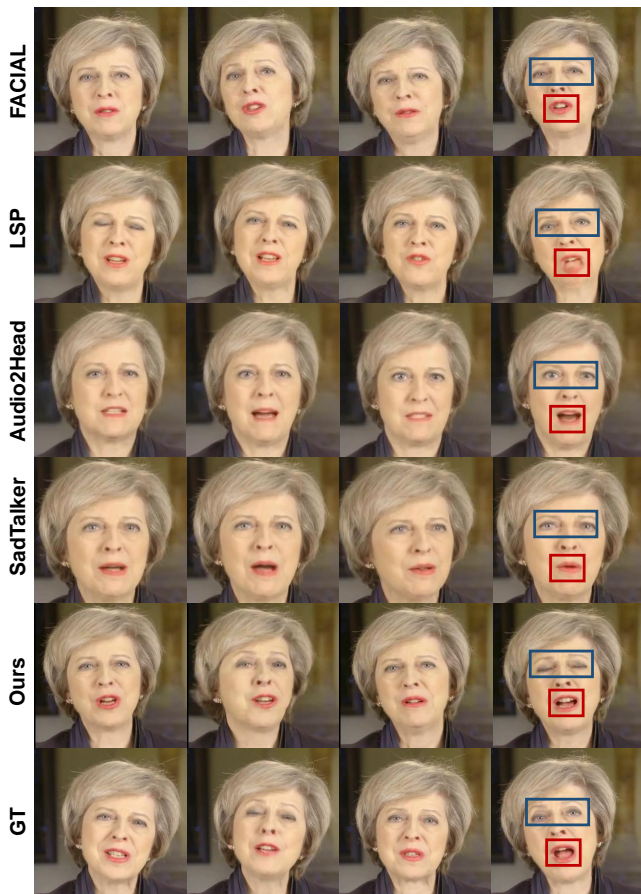


Fig. 7. Qualitative comparison for motion-controllable talking video portraits on the one test sample from LSP [20]. From top to bottom: FACIAL [21], LSP [20], Audio2Head [22], SadTalker [56], ours, and ground truth.

expression and the smoothness of the emotional transition video, we introduce two new metrics inspired by [74], [81]:

(1) Emotion perceptual path length (**E-PPL**, \downarrow): We train a VGGNet [82] for emotion classification on the MEAD dataset to make the network more focused on emotion. Then, we calculate the mean perceptual loss between adjacent images in 17-frame sequences using the trained VGGNet. This metric serves as an indicator of the emotional smoothness and consistency of the generated transition video.

(2) Emotion perceptual distance variance (**E-PDV**, \downarrow): Similarly, we compute the perceptual loss between adjacent images in 17-frame sequences and then calculate the variance of these distances in the sequence. This serves as a natural measure of the homogeneity of the emotion video transition rate.

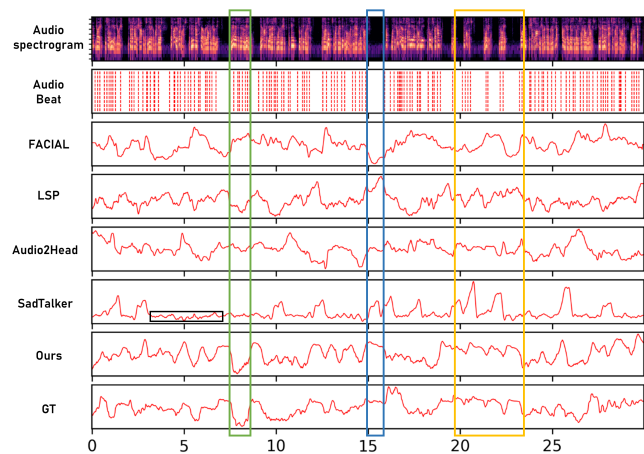


Fig. 8. Comparison of head motion on the test video sample from LSP [20]. From top to bottom: the audio spectrogram, audio beat, FACIAL [21], LSP [20], Audio2Head [22], SadTalker [56], ours, and ground truth.

Besides, we adopt the SyncNet score to evaluate the audio-visual synchronization of the generated emotional transition video. The quantitative results of all approaches are presented in Table III. Our methods achieve significantly lower **E-PPL** and **E-PDV** than others, showing smoother emotion transitions. On the other hand, our GMTalker has a higher Sync score, demonstrating more accurate lip synchronization when the emotions are changed.

Comparison of Motion Generation. We compare our approach with several state-of-arts pose-controllable methods on five test video samples from LSP. As depicted in Table IV, our method shows outstanding performance in terms of **Div**, **BA**, and **PCM**. Meanwhile, we also achieve the best performance on overall visual quality and lip sync metrics. This suggests that the latent space learned by normalizing flow can represent complex motion distributions derived from pretrained models. Qualitative comparisons are shown in Fig 7. Our approach excels in generating diverse head motions, natural eye blinks, and accurate mouth shapes with audio, and visual quality compared with other methods.

To comprehensively evaluate motion diversity and its correlation with audio, we utilize correlation map [22] to compare our method with several motion-controllable methods. We reduce the 3-dimensional head motion embeddings into one dimension by PCA following [22]. As depicted in Fig 8, existing methods struggle to generate realistic head movements consistent with rhythmic audio beats. In the case of silence audio (shown in the blue boxes), the head motion should

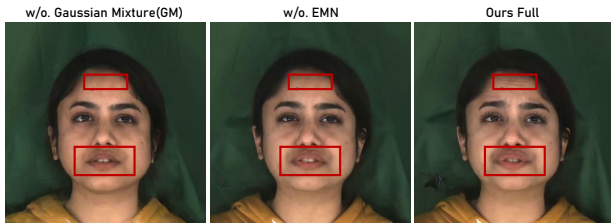


Fig. 9. Qualitative results of ablation study for Gaussian mixture (GM) prior and EMN. From left to right, the results are w/o GM, with GM but w/o EMN, and our full model.

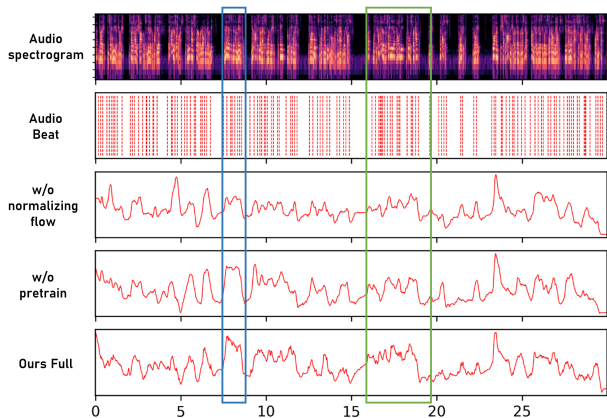


Fig. 10. Qualitative results of ablation study for normalizing flow motion generator. From top to bottom: audio spectrogram, audio beat, the head motion beat w/o normalizing flow, w/o pre-train, and our full results.

remain static intuitively, yet their generated head motion often exhibits dynamic fluctuations. Conversely, in the case of speaking audio (shown in the green boxes), the head motion should synchronize with the audio, but their generated head motion may remain static and lack rich changes. In contrast, our head motions preserve the rhythm and synchronization with audio, and are much closer to the ground truth, as shown in the yellow boxes.

C. User Study

To further quantify the quality of generated video portraits, we conduct a user study to compare real data with generated ones from some representative methods: MakeItTalk [38], Styletalk [11], EVP [5], EAT [16]. We randomly select overall 24 audio clips (3 clips \times 8 emotions) from the test set of MEAD to generate video samples for each method. The 14 recruited participants are required to evaluate the given video from three aspects “lip synchronization”, “video quality”, and “emotion accuracy” and choose the top two preferred videos for each of these aspects from all the methods presented. The results are shown in Table VII. Our approach achieves the best scores for lip-sync, video quality, and emotion accuracy, indicating the expressiveness of our GMEG, NFMG, and emotion-guided head generator with EMN.

D. Ablation Study

To demonstrate the effectiveness of our designed choice, we perform ablation studies with the following three alternative modules: 1) w/o Gaussian mixture prior in GMEG, where

TABLE V
QUANTITATIVE ABLATION STUDY RESULTS FOR GMEG AND EMN.

Ablation	PSNR/SSIM \uparrow	FID \downarrow	M/F-LMD \downarrow	Sync \uparrow	Acc_{emo} \uparrow
w/o GM	23.71/0.77	14.64	1.61/1.85	7.23	65.61
w/o EMN	24.82/0.78	12.95	1.62/1.81	7.30	72.33
Ours Full	25.18/0.81	11.86	1.52/1.76	7.41	77.73

TABLE VI
QUANTITATIVE RESULTS OF THE ABLATION STUDY FOR NORMALIZING FLOW MOTION GENERATOR ON TEST SAMPLES FROM LSP.

Ablation	BA \uparrow	Div \uparrow	PCM \uparrow
w/o normalizing flow	0.244	2.101	0.427
w/o pre-train	0.272	2.189	0.438
Ours Full	0.293	2.223	0.447

we replace the Gaussian mixture distribution prior with a unimodal Gaussian prior, 2) w/o EMN, where we use 4-layers MLP as mapping network without emotion-guided, 3) w/o normalization flow, where we use the normal distribution as the prior of the motion generator.

a) *The Ablation of GMEG and EMN:* We conduct the ablation of GMEG and EMN on the MEAD test set. We compare the visual quality, audio-visual synchronization, and emotional accuracy metrics before and after removing the Gaussian mixture prior in GMEG and EMN, respectively. As shown in Table V, all components can improve video quality and emotion accuracy. In particular, when removing the constraints on the Gaussian mixture distribution, there is a significant decline in the emotional accuracy of the generated videos, demonstrating the effectiveness of our disentangled emotion latent space. A qualitative case in generating “Fear” expression is illustrated in Fig 9. It can be observed that when replacing the Gaussian mixture distribution with normalization distribution or removing the EMN module, the model can hardly generate the desired expression and facial details, including wrinkles, mouth shapes, and eye gaze. In contrast, by incorporating the Gaussian mixture and EMN, our method can generate more faithful emotion as well as better visual quality and audio-lip synchronization.

b) *The Ablation of NFMG:* For the ablation of NFMG, we focus on the Div, BA, and PCM metrics. As shown in Table VI, the quantitative results demonstrate that our normalizing flow with pre-training can provide richness motion prior and generate diverse and wide-range motions. Moreover, we conduct a perceptual study to evaluate the correlation between generated head motion and audio beat. As depicted in Fig 10, the head movements generated by our full model exhibit greater rhythm and synchronization with the audio beat, while also showing increased diversity.

E. Disentanglement Analysis

To better validate the disentangling of our GMEG, we feed the same input speech and different emotion labels into GMEG. As shown in Fig 11, the mouth movements in the generated video correspond to the speech, while the facial expression matches the target emotion label. Moreover, to evaluate the disentanglement of various emotions in our Gaussian mixture latent space, we use t-SNE [83] to visualize the latent codes. Illustrated in Fig 12, different colors



Fig. 11. Additional emotional portraits generated by our GMTalker. Given the same input audio, we can generate high-fidelity and faithful emotional expressions according to the target emotion label. The identities are from the MEAD dataset.

TABLE VII

USER STUDY ON MEAD DATASETS. THE TABLE DISPLAYS THE PERCENTAGE OF PARTICIPANTS’ PREFERENCES FOR EACH METHOD IN TERMS OF EACH ASPECT.

Method	MakeltTalk	Styletalk	EVP	EAT	GMTalker	GT
Visual Quality	4.19	5.18	10.35	6.99	35.38	37.91
Audio-visual Sync	7.92	6.13	5.08	12.41	29.45	39.01
Emotion Accuracy	4.46	5.94	4.75	10.55	34.77	39.52

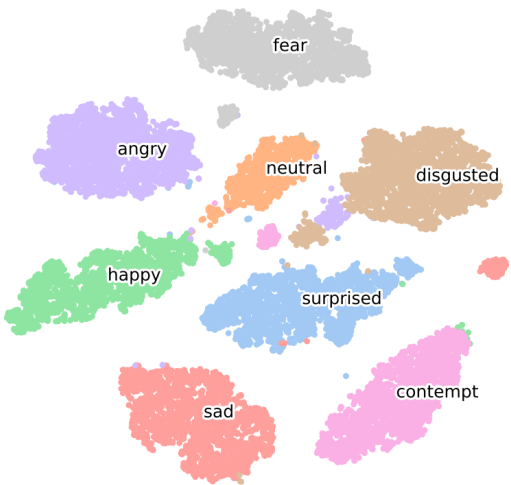


Fig. 12. T-SNE visualization of Gaussian mixture latent space. Different colors indicate different emotion types.

represent sampled latent code with eight different emotion categories. By using the Gaussian mixture distribution, the samples sharing the same emotion are clustered together, while those with different emotions are distinctly separated. This indicates the contribution of the proposed GMEG in effectively disentangling various emotions from each other.

V. DISCUSSION AND CONCLUSION

a) Limitation: Although our method has demonstrated its superiority compared with existing emotional talking video portrait methods, there are still several limitations: (1) our method relies on high-quality videos containing rich emotional content, the capturing of which comes with certain challenges; (2) our method still describes limited emotions subjecting to the eight categories in the dataset and need to train on the target person.

b) Potential Social Impact: As our method is capable of producing realistic emotional talking portraits from monocular videos, there is a potential for its application in creating deceptive talking videos, which should be addressed carefully before its deployment.

c) Conclusion: In this paper, we present GMTalker which can generate high-fidelity and faithful emotional talking video portraits with diverse motions. To achieve precise emotion control and continuous emotion transition, we propose the GMEG to construct a continuous and disentangled Gaussian mixture latent space. Then, NFMG is proposed to alleviate the “mean motion” problem and predict diverse motions, including head poses, eye blinks, and gazes. Finally, we introduce an emotion-guided head generator with the proposed EMN to generate high-quality emotional talking video portraits with personalized speaking styles. By incorporating GMEG, NFMG, EMN, and the personalized head generator, our method offers a unique blend of advantages, combining faithful and smooth emotion interpolation, diverse head and eye motions, and high-quality video generation. Overall, experiments have demonstrated that our method outperforms other state-of-the-art approaches, and we believe that our Gaussian mixture latent space will inspire future research on talking head generation.

REFERENCES

- [1] K. Prajwal, R. Mukhopadhyay, V. P. Namboodiri, and C. Jawahar, "A lip sync expert is all you need for speech to lip generation in the wild," in *Proceedings of the 28th ACM international conference on multimedia*, 2020, pp. 484–492. [1](#), [2](#), [7](#), [8](#), [9](#)
- [2] Y. Sun, H. Zhou, K. Wang, Q. Wu, Z. Hong, J. Liu, E. Ding, J. Wang, Z. Liu, and K. Hideki, "Masked lip-sync prediction by audio-visual contextual exploitation in transformers," in *SIGGRAPH Asia 2022 Conference Papers*, 2022, pp. 1–9. [1](#), [2](#)
- [3] K. Cheng, X. Cun, Y. Zhang, M. Xia, F. Yin, M. Zhu, X. Wang, J. Wang, and N. Wang, "Videoretalking: Audio-based lip synchronization for talking head video editing in the wild," in *SIGGRAPH Asia 2022 Conference Papers*, 2022, pp. 1–9. [1](#), [2](#)
- [4] J. Guan, Z. Zhang, H. Zhou, T. Hu, K. Wang, D. He, H. Feng, J. Liu, E. Ding, Z. Liu *et al.*, "Stylesync: High-fidelity generalized and personalized lip sync in style-based generator," in *Proceedings of the IEEE/CVF Conference on Computer Vision and Pattern Recognition*, 2023, pp. 1505–1515. [1](#), [2](#)
- [5] X. Ji, H. Zhou, K. Wang, W. Wu, C. C. Loy, X. Cao, and F. Xu, "Audio-driven emotional video portraits," in *Proceedings of the IEEE/CVF conference on computer vision and pattern recognition*, 2021, pp. 14 080–14 089. [1](#), [3](#), [7](#), [11](#)
- [6] S. Tan, B. Ji, and Y. Pan, "Emmn: Emotional motion memory network for audio-driven emotional talking face generation," in *Proceedings of the IEEE/CVF International Conference on Computer Vision*, 2023, pp. 22 146–22 156. [1](#), [3](#)
- [7] C. Xu, J. Zhu, J. Zhang, Y. Han, W. Chu, Y. Tai, C. Wang, Z. Xie, and Y. Liu, "High-fidelity generalized emotional talking face generation with multi-modal emotion space learning," in *Proceedings of the IEEE/CVF Conference on Computer Vision and Pattern Recognition*, 2023, pp. 6609–6619. [1](#)
- [8] X. Ji, H. Zhou, K. Wang, Q. Wu, W. Wu, F. Xu, and X. Cao, "Eamm: One-shot emotional talking face via audio-based emotion-aware motion model," in *ACM SIGGRAPH 2022 Conference Proceedings*, 2022, pp. 1–10. [1](#), [3](#), [7](#), [8](#)
- [9] B. Liang, Y. Pan, Z. Guo, H. Zhou, Z. Hong, X. Han, J. Han, J. Liu, E. Ding, and J. Wang, "Expressive talking head generation with granular audio-visual control," in *Proceedings of the IEEE/CVF Conference on Computer Vision and Pattern Recognition*, 2022, pp. 3387–3396. [1](#), [3](#)
- [10] D. Wang, Y. Deng, Z. Yin, H.-Y. Shum, and B. Wang, "Progressive disentangled representation learning for fine-grained controllable talking head synthesis," in *Proceedings of the IEEE/CVF Conference on Computer Vision and Pattern Recognition*, 2023, pp. 17 979–17 989. [1](#), [3](#), [7](#), [8](#), [9](#)
- [11] Y. Ma, S. Wang, Z. Hu, C. Fan, T. Lv, Y. Ding, Z. Deng, and X. Yu, "Styletalk: One-shot talking head generation with controllable speaking styles," *arXiv preprint arXiv:2301.01081*, 2023. [1](#), [2](#), [3](#), [7](#), [8](#), [9](#), [11](#)
- [12] S. E. Eskimez, Y. Zhang, and Z. Duan, "Speech driven talking face generation from a single image and an emotion condition," *IEEE Transactions on Multimedia*, vol. 24, pp. 3480–3490, 2021. [1](#), [3](#), [7](#), [8](#), [9](#)
- [13] K. Wang, Q. Wu, L. Song, Z. Yang, W. Wu, C. Qian, R. He, Y. Qiao, and C. C. Loy, "Mead: A large-scale audio-visual dataset for emotional talking-face generation," in *European Conference on Computer Vision*. Springer, 2020, pp. 700–717. [1](#), [3](#), [6](#), [8](#)
- [14] S. Sinha, S. Biswas, R. Yadav, and B. Bhowmick, "Emotion-controllable generalized talking face generation," *arXiv preprint arXiv:2205.01155*, 2022. [1](#), [3](#)
- [15] S. Gururani, A. Mallya, T.-C. Wang, R. Valle, and M.-Y. Liu, "Space: Speech-driven portrait animation with controllable expression," in *Proceedings of the IEEE/CVF International Conference on Computer Vision*, 2023, pp. 20 914–20 923. [1](#), [3](#)
- [16] Y. Gan, Z. Yang, X. Yue, L. Sun, and Y. Yang, "Efficient emotional adaptation for audio-driven talking-head generation," in *Proceedings of the IEEE/CVF International Conference on Computer Vision*, 2023, pp. 22 634–22 645. [1](#), [3](#), [7](#), [8](#), [9](#), [11](#)
- [17] L. Chen, G. Cui, C. Liu, Z. Li, Z. Kou, Y. Xu, and C. Xu, "Talking-head generation with rhythmic head motion," in *European Conference on Computer Vision*. Springer, 2020, pp. 35–51. [1](#), [2](#)
- [18] R. Yi, Z. Ye, J. Zhang, H. Bao, and Y.-J. Liu, "Audio-driven talking face video generation with learning-based personalized head pose," *arXiv preprint arXiv:2002.10137*, 2020. [1](#), [2](#)
- [19] H. Zhou, Y. Sun, W. Wu, C. C. Loy, X. Wang, and Z. Liu, "Pose-controllable talking face generation by implicitly modularized audio-visual representation," in *Proceedings of the IEEE/CVF conference on computer vision and pattern recognition*, 2021, pp. 4176–4186. [1](#), [2](#)
- [20] Y. Lu, J. Chai, and X. Cao, "Live speech portraits: real-time photorealistic talking-head animation," *ACM Transactions on Graphics (TOG)*, vol. 40, no. 6, pp. 1–17, 2021. [1](#), [2](#), [7](#), [10](#)
- [21] C. Zhang, Y. Zhao, Y. Huang, M. Zeng, S. Ni, M. Budagavi, and X. Guo, "Facial: Synthesizing dynamic talking face with implicit attribute learning," in *Proceedings of the IEEE/CVF international conference on computer vision*, 2021, pp. 3867–3876. [1](#), [2](#), [7](#), [10](#)
- [22] S. Wang, L. Li, Y. Ding, C. Fan, and X. Yu, "Audio2head: Audio-driven one-shot talking-head generation with natural head motion," *arXiv preprint arXiv:2107.09293*, 2021. [1](#), [2](#), [7](#), [10](#)
- [23] S. Wang, L. Li, Y. Ding, and X. Yu, "One-shot talking face generation from single-speaker audio-visual correlation learning," in *Proceedings of the AAAI Conference on Artificial Intelligence*, vol. 36, no. 3, 2022, pp. 2531–2539. [1](#), [2](#), [7](#), [8](#), [9](#)
- [24] Y. Liu, L. Lin, F. Yu, C. Zhou, and Y. Li, "Moda: Mapping-once audio-driven portrait animation with dual attentions," in *Proceedings of the IEEE/CVF International Conference on Computer Vision*, 2023, pp. 23 020–23 029. [1](#), [2](#)
- [25] Z. Yu, Z. Yin, D. Zhou, D. Wang, F. Wong, and B. Wang, "Talking head generation with probabilistic audio-to-visual diffusion priors," in *Proceedings of the IEEE/CVF International Conference on Computer Vision*, 2023, pp. 7645–7655. [1](#)
- [26] J. S. Chung, A. Nagrani, and A. Zisserman, "Voxceleb2: Deep speaker recognition," *arXiv preprint arXiv:1806.05622*, 2018. [1](#), [6](#), [7](#)
- [27] L. Wang, Z. Chen, T. Yu, C. Ma, L. Li, and Y. Liu, "Faceverse: a fine-grained and detail-controllable 3d face morphable model from a hybrid dataset," in *Proceedings of the IEEE/CVF conference on computer vision and pattern recognition*, 2022, pp. 20 333–20 342. [1](#), [2](#), [3](#)
- [28] L. Wang, X. Zhao, J. Sun, Y. Zhang, H. Zhang, T. Yu, and Y. Liu, "Styleavatar: Real-time photo-realistic portrait avatar from a single video," *arXiv preprint arXiv:2305.00942*, 2023. [1](#), [3](#), [6](#), [7](#)
- [29] T. Karras, T. Aila, S. Laine, A. Herva, and J. Lehtinen, "Audio-driven facial animation by joint end-to-end learning of pose and emotion," *ACM Transactions on Graphics (TOG)*, vol. 36, no. 4, pp. 1–12, 2017. [2](#)
- [30] A. Richard, M. Zollhöfer, Y. Wen, F. De la Torre, and Y. Sheikh, "Meshtalk: 3d face animation from speech using cross-modality disentanglement," in *Proceedings of the IEEE/CVF International Conference on Computer Vision*, 2021, pp. 1173–1182. [2](#)
- [31] Y. Fan, Z. Lin, J. Saito, W. Wang, and T. Komura, "Faceformer: Speech-driven 3d facial animation with transformers," in *Proceedings of the IEEE/CVF Conference on Computer Vision and Pattern Recognition*, 2022, pp. 18 770–18 780. [2](#), [4](#)
- [32] J. Xing, M. Xia, Y. Zhang, X. Cun, J. Wang, and T.-T. Wong, "Codetalker: Speech-driven 3d facial animation with discrete motion prior," in *Proceedings of the IEEE/CVF Conference on Computer Vision and Pattern Recognition*, 2023, pp. 12 780–12 790. [2](#)
- [33] B. Thambiraja, I. Habibie, S. Aliakbarian, D. Cosker, C. Theobalt, and J. Thies, "Imitator: Personalized speech-driven 3d facial animation," in *Proceedings of the IEEE/CVF International Conference on Computer Vision*, 2023, pp. 20 621–20 631. [2](#)
- [34] Z. Peng, H. Wu, Z. Song, H. Xu, X. Zhu, J. He, H. Liu, and Z. Fan, "Emotalk: Speech-driven emotional disentanglement for 3d face animation," in *Proceedings of the IEEE/CVF International Conference on Computer Vision*, 2023, pp. 20 687–20 697. [2](#)
- [35] R. Daněček, K. Chhatre, S. Tripathi, Y. Wen, M. J. Black, and T. Bolkart, "Emotional speech-driven animation with content-emotion disentanglement," *arXiv preprint arXiv:2306.08990*, 2023. [2](#)
- [36] S. Suwajanakorn, S. M. Seitz, and I. Kemelmacher-Shlizerman, "Synthesizing obama: learning lip sync from audio," *ACM Transactions on Graphics (ToG)*, vol. 36, no. 4, pp. 1–13, 2017. [2](#)
- [37] L. Chen, R. K. Maddox, Z. Duan, and C. Xu, "Hierarchical cross-modal talking face generation with dynamic pixel-wise loss," in *Proceedings of the IEEE/CVF conference on computer vision and pattern recognition*, 2019, pp. 7832–7841. [2](#), [8](#)
- [38] Y. Zhou, X. Han, E. Shechtman, J. Echevarria, E. Kalogerakis, and D. Li, "Makeltalk: speaker-aware talking-head animation," *ACM Transactions On Graphics (TOG)*, vol. 39, no. 6, pp. 1–15, 2020. [2](#), [7](#), [8](#), [11](#)
- [39] P. KR, R. Mukhopadhyay, J. Philip, A. Jha, V. Namboodiri, and C. Jawahar, "Towards automatic face-to-face translation," in *Proceedings of the 27th ACM international conference on multimedia*, 2019, pp. 1428–1436. [2](#)
- [40] S. J. Park, M. Kim, J. Hong, J. Choi, and Y. M. Ro, "Synctalkface: Talking face generation with precise lip-syncing via audio-lip memory," in *Proceedings of the AAAI Conference on Artificial Intelligence*, vol. 36, no. 2, 2022, pp. 2062–2070. [2](#)
- [41] T. Ki and D. Min, "Stylelipsync: Style-based personalized lip-sync video generation," *arXiv preprint arXiv:2305.00521*, 2023. [2](#)

- [42] Z. Zhang, Z. Hu, W. Deng, C. Fan, T. Lv, and Y. Ding, "Dinet: Deformation inpainting network for realistic face visually dubbing on high resolution video," *arXiv preprint arXiv:2303.03988*, 2023. **2**
- [43] X. Wu, P. Hu, Y. Wu, X. Lyu, Y.-P. Cao, Y. Shan, W. Yang, Z. Sun, and X. Qi, "Speech2lip: High-fidelity speech to lip generation by learning from a short video," in *Proceedings of the IEEE/CVF International Conference on Computer Vision*, 2023, pp. 22 168–22 177. **2**
- [44] J. Wang, X. Qian, M. Zhang, R. T. Tan, and H. Li, "Seeing what you said: Talking face generation guided by a lip reading expert," in *Proceedings of the IEEE/CVF Conference on Computer Vision and Pattern Recognition*, 2023, pp. 14 653–14 662. **2**
- [45] S. Shen, W. Zhao, Z. Meng, W. Li, Z. Zhu, J. Zhou, and J. Lu, "Diffstalk: Crafting diffusion models for generalized audio-driven portraits animation," in *Proceedings of the IEEE/CVF Conference on Computer Vision and Pattern Recognition*, 2023, pp. 1982–1991. **2**
- [46] J. S. Chung and A. Zisserman, "Out of time: automated lip sync in the wild," in *Computer Vision—ACCV 2016 Workshops: ACCV 2016 International Workshops, Taipei, Taiwan, November 20–24, 2016, Revised Selected Papers, Part II 13*. Springer, 2017, pp. 251–263. **2, 8**
- [47] Z. Zhang, L. Li, Y. Ding, and C. Fan, "Flow-guided one-shot talking face generation with a high-resolution audio-visual dataset," in *Proceedings of the IEEE/CVF Conference on Computer Vision and Pattern Recognition*, 2021, pp. 3661–3670. **2**
- [48] H. Zhou, Y. Liu, Z. Liu, P. Luo, and X. Wang, "Talking face generation by adversarially disentangled audio-visual representation," in *Proceedings of the AAAI conference on artificial intelligence*, vol. 33, no. 01, 2019, pp. 9299–9306. **2**
- [49] Y. Sun, H. Zhou, Z. Liu, and H. Koike, "Speech2talking-face: Inferring and driving a face with synchronized audio-visual representation," in *IJCAI*, vol. 2, 2021, p. 4. **2**
- [50] J. Wang, K. Zhao, S. Zhang, Y. Zhang, Y. Shen, D. Zhao, and J. Zhou, "Lipformer: High-fidelity and generalizable talking face generation with a pre-learned facial codebook," in *Proceedings of the IEEE/CVF Conference on Computer Vision and Pattern Recognition*, 2023, pp. 13 844–13 853. **2**
- [51] Y. Deng, J. Yang, S. Xu, D. Chen, Y. Jia, and X. Tong, "Accurate 3d face reconstruction with weakly-supervised learning: From single image to image set," in *Proceedings of the IEEE/CVF conference on computer vision and pattern recognition workshops*, 2019, pp. 0–0. **2, 3**
- [52] D. Das, S. Biswas, S. Sinha, and B. Bhowmick, "Speech-driven facial animation using cascaded gans for learning of motion and texture," in *Computer Vision—ECCV 2020: 16th European Conference, Glasgow, UK, August 23–28, 2020, Proceedings, Part XXX 16*. Springer, 2020, pp. 408–424. **2**
- [53] W. Zhong, C. Fang, Y. Cai, P. Wei, G. Zhao, L. Lin, and G. Li, "Identity-preserving talking face generation with landmark and appearance priors," in *Proceedings of the IEEE/CVF Conference on Computer Vision and Pattern Recognition*, 2023, pp. 9729–9738. **2**
- [54] J. Thies, M. Elgharib, A. Tewari, C. Theobalt, and M. Nießner, "Neural voice puppetry: Audio-driven facial reenactment," in *Computer Vision—ECCV 2020: 16th European Conference, Glasgow, UK, August 23–28, 2020, Proceedings, Part XVI 16*. Springer, 2020, pp. 716–731. **2**
- [55] L. Song, W. Wu, C. Qian, R. He, and C. C. Loy, "Everybody's talkin': Let me talk as you want," *IEEE Transactions on Information Forensics and Security*, vol. 17, pp. 585–598, 2022. **2**
- [56] W. Zhang, X. Cun, X. Wang, Y. Zhang, X. Shen, Y. Guo, Y. Shan, and F. Wang, "Sadtalker: Learning realistic 3d motion coefficients for stylized audio-driven single image talking face animation," in *Proceedings of the IEEE/CVF Conference on Computer Vision and Pattern Recognition*, 2023, pp. 8652–8661. **2, 3, 5, 7, 8, 10**
- [57] L. Tian, Q. Wang, B. Zhang, and L. Bo, "Emo: Emote portrait alive-generating expressive portrait videos with audio2video diffusion model under weak conditions," *arXiv preprint arXiv:2402.17485*, 2024. **3**
- [58] P. Paysan, R. Knothe, B. Amberg, S. Romdhani, and T. Vetter, "A 3d face model for pose and illumination invariant face recognition," in *2009 sixth IEEE international conference on advanced video and signal based surveillance*. Ieee, 2009, pp. 296–301. **3**
- [59] T. Li, T. Bolkart, M. J. Black, H. Li, and J. Romero, "Learning a model of facial shape and expression from 4d scans," *ACM Trans. Graph.*, vol. 36, no. 6, pp. 194–1, 2017. **3**
- [60] Y. Ren, G. Li, Y. Chen, T. H. Li, and S. Liu, "Pirenderer: Controllable portrait image generation via semantic neural rendering," in *Proceedings of the IEEE/CVF International Conference on Computer Vision*, 2021, pp. 13 759–13 768. **3**
- [61] W.-N. Hsu, B. Bolte, Y.-H. H. Tsai, K. Lakhotia, R. Salakhutdinov, and A. Mohamed, "Hubert: Self-supervised speech representation learning by masked prediction of hidden units," *IEEE/ACM Transactions on Audio, Speech, and Language Processing*, vol. 29, pp. 3451–3460, 2021. **3**
- [62] Z. Ye, Z. Jiang, Y. Ren, J. Liu, J. He, and Z. Zhao, "Geneface: Generalized and high-fidelity audio-driven 3d talking face synthesis," *arXiv preprint arXiv:2301.13430*, 2023. **3, 5**
- [63] Z. Ye, T. Zhong, Y. Ren, J. Yang, W. Li, J. Huang, Z. Jiang, J. He, R. Huang, J. Liu *et al.*, "Real3d-portrait: One-shot realistic 3d talking portrait synthesis," *arXiv preprint arXiv:2401.08503*, 2024. **3**
- [64] K. Sohn, H. Lee, and X. Yan, "Learning structured output representation using deep conditional generative models," *Advances in neural information processing systems*, vol. 28, 2015. **3**
- [65] D. P. Kingma and M. Welling, "Auto-encoding variational bayes," *arXiv preprint arXiv:1312.6114*, 2013. **4**
- [66] A. Vaswani, N. Shazeer, N. Parmar, J. Uszkoreit, L. Jones, A. N. Gomez, L. Kaiser, and I. Polosukhin, "Attention is all you need," *Advances in neural information processing systems*, vol. 30, 2017. **4**
- [67] N. Dilokthanakul, P. A. Mediano, M. Garnelo, M. C. Lee, H. Salimbeni, K. Arulkumaran, and M. Shanahan, "Deep unsupervised clustering with gaussian mixture variational autoencoders," *arXiv preprint arXiv:1611.02648*, 2016. **4**
- [68] D. Rezende and S. Mohamed, "Variational inference with normalizing flows," in *International conference on machine learning*. PMLR, 2015, pp. 1530–1538. **5**
- [69] Y. Ren, J. Liu, and Z. Zhao, "Portaspeech: Portable and high-quality generative text-to-speech," *Advances in Neural Information Processing Systems*, vol. 34, pp. 13 963–13 974, 2021. **5, 6**
- [70] G. E. Henter, S. Alexanderson, and J. Beskow, "Moglow: Probabilistic and controllable motion synthesis using normalising flows," *ACM Transactions on Graphics (TOG)*, vol. 39, no. 6, pp. 1–14, 2020. **6**
- [71] D. P. Kingma and P. Dhariwal, "Glow: Generative flow with invertible 1x1 convolutions," *Advances in neural information processing systems*, vol. 31, 2018. **6**
- [72] S.-g. Lee, S. Kim, and S. Yoon, "Nanoflow: Scalable normalizing flows with sublinear parameter complexity," *Advances in Neural Information Processing Systems*, vol. 33, pp. 14 058–14 067, 2020. **6**
- [73] Y. Choi, Y. Uh, J. Yoo, and J.-W. Ha, "Stargan v2: Diverse image synthesis for multiple domains," in *Proceedings of the IEEE/CVF conference on computer vision and pattern recognition*, 2020, pp. 8188–8197. **6**
- [74] T. Karras, S. Laine, M. Aittala, J. Hellsten, J. Lehtinen, and T. Aila, "Analyzing and improving the image quality of stylegan," in *Proceedings of the IEEE/CVF conference on computer vision and pattern recognition*, 2020, pp. 8110–8119. **6, 10**
- [75] H. Cao, D. G. Cooper, M. K. Keutmann, R. C. Gur, A. Nenkova, and R. Verma, "Crema-d: Crowd-sourced emotional multimodal actors dataset," *IEEE transactions on affective computing*, vol. 5, no. 4, pp. 377–390, 2014. **6, 8, 9**
- [76] K. Vougioukas, S. Petridis, and M. Pantic, "Realistic speech-driven facial animation with gans," *International Journal of Computer Vision*, vol. 128, no. 5, pp. 1398–1413, 2020. **7, 8**
- [77] M. Stypulkowski, K. Vougioukas, S. He, M. Zięba, S. Petridis, and M. Pantic, "Diffused heads: Diffusion models beat gans on talking-face generation," in *Proceedings of the IEEE/CVF Winter Conference on Applications of Computer Vision*, 2024, pp. 5091–5100. **7, 8, 9**
- [78] H. Liu, Z. Zhu, N. Iwamoto, Y. Peng, Z. Li, Y. Zhou, E. Bozkurt, and B. Zheng, "Beat: A large-scale semantic and emotional multi-modal dataset for conversational gestures synthesis," in *European conference on computer vision*. Springer, 2022, pp. 612–630. **8**
- [79] C. Zhang, H. Liu, Y. Deng, B. Xie, and Y. Li, "Tokenhpe: Learning orientation tokens for efficient head pose estimation via transformers," in *Proceedings of the IEEE/CVF Conference on Computer Vision and Pattern Recognition*, 2023, pp. 8897–8906. **8**
- [80] L. Siyao, W. Yu, T. Gu, C. Lin, Q. Wang, C. Qian, C. C. Loy, and Z. Liu, "Bailando: 3d dance generation by actor-critic gpt with choreographic memory," in *Proceedings of the IEEE/CVF Conference on Computer Vision and Pattern Recognition*, 2023, pp. 11 050–11 059. **8**
- [81] K. Zhang, Y. Zhou, X. Xu, X. Pan, and B. Dai, "Diffmorpher: Unleashing the capability of diffusion models for image morphing," *arXiv preprint arXiv:2312.07409*, 2023. **10**
- [82] K. Simonyan and A. Zisserman, "Very deep convolutional networks for large-scale image recognition," *arXiv preprint arXiv:1409.1556*, 2014. **10**
- [83] L. Van der Maaten and G. Hinton, "Visualizing data using t-sne," *Journal of machine learning research*, vol. 9, no. 11, 2008. **11**